J. Pharm. Pharmacol. 1985, 37: 521–527
Received February 4, 1985

Physicochemical properties of endotoxins in large volume parenterals

C. BAGGERMAN*, C. PATHMAMANOHARAN†, F. SPIES‡, J. G. H. JOOSTEN§ AND H. E. JUNGINGER§

*Central Laboratory of the Netherlands Red Cross Blood Transfusion Service, PO Box 9406, 1006 AK Amsterdam, †Van 't Hoff Laboratory for Colloid Chemistry, State University Utrecht, Utrecht, ‡Psychiatric Hospital Endegeest, Dept. of Electronmicroscopy, Oegstgeest, §Dept. of Pharmaceutical Technology, State University of Leiden, Leiden, The Netherlands.

Endotoxins of *Escherichia coli*, *Salmonella abortus equi* and *Serratia marcescens* were examined using freeze-etch electronmicroscopy and light scattering techniques, with emphasis on their aggregation state. These endotoxins show distinct features of particle size and mass and they may be affected by the presence or absence of Ca^{2+} ions. No important differences were observed in the particle characteristics of the respective endotoxins in various infusion fluids.

Endotoxins, the outer cell-wall fragments of Gram-negative bacteria, may be responsible for pyrogenic reactions if they occur in sufficient amounts in large volume parenterals (infusion fluids). Both raw materials (Baggerman & Kannegieter 1984) and inadequate manufacturing procedures (Maki 1976) might contribute to this. Endotoxins are believed not to be merely monomolecular structures, but rather vesicular or micellar aggregates of lipopolysaccharide molecules (Hannecart-Pokorni et al 1973; Sweadner et al 1977). However, different states of aggregation have been described for endotoxins depending on the medium. Divalent cations and detergents seem to modify this state of aggregation (Ribi et al 1966; DePamphilis 1971; Sweadner et al 1977). Changes in aggregation state have direct implications for the pyrogenic activity of endotoxins, because subunits have been shown not to exhibit such activity (Ribi et al 1966).

The composition of the solution affected the removal of endotoxins from large volume parenterals (LVP) by depth-filtration (Woog et al 1977; Baggerman et al 1981). The quantitative detection of endotoxins in LVPs using the Limulus Amoebocyte Lysate-Chromogenic Substrate (LAL-CS) method is also influenced by composition (Tsuji & Steindler 1983; Kannegieter & Baggerman 1984). Both these phenomena might be explained if endotoxins in large volume parenterals occur in different aggregation states.

The aim of this study was to investigate whether different aggregation states exist in different LVPs.

* Correspondence.

MATERIALS AND METHODS

Lipopolysaccharides (Sigma Chemicals), prepared by phenolic extraction of *Escherichia coli*, serotype 0111:B4, *Salmonella abortus equi* and *Serratia marcescens* were used with LVPs and sterile, pyrogen-free water for injections, prepared in our hospital pharmacy except Vamin-N (Kabi, Sweden) and Isodex (Organon Teknika, The Netherlands). Sterile, pyrogen-free 0·1 M EDTA and $CaCl_2$ solutions were included for comparison.

Solutions for light scattering experiments and electronmicroscopy were prepared as follows. LVPs were filtered through 0·025 μm membrane filters (Millipore VSWP 04700). Endotoxins were dispersed in these solutions and filtered through 0·22 μm membrane filters (Van Leer Medical VV 036). Various amounts of these stock solutions were added to the corresponding filtered infusion fluids to obtain a series of five concentrations. Both stock solutions and dilutions were stored for no longer than three days; storage up to three weeks at 4 °C did not affect the particle size of the endotoxins as shown by light scattering. The 0·22 μm filtration affected neither the endotoxin content of the solutions measured by LAL-CS detection nor the particle size of the endotoxins. For light scattering experiments, the lowest possible concentration ranges were chosen i.e. 20–100 μg ml^{-1} for *E. coli* and *S. abortus equi* endotoxin and 100–500 μg ml^{-1} for *S. marcesens* endotoxin. For 0·1 M EDTA, all the endotoxins were in the range 100–500 μg ml^{-1}. The concentrations used for refractive index-increment measurements, were 0·8, 1·2, 1·6 and 2 mg ml^{-1} and for electronmicroscopy experiments the solutions contained 5 or 10 mg ml^{-1}.

Freeze-etch electronmicroscopy

Small drops of endotoxin dispersions were transferred into silver specimen holders (see Wisse & Spies 1981), which were quenched in soiid/liquid Freon 22. The frozen specimens were fractured and etched in a Balzers BAF 400 at 10^{-6} torr and -100 °C during 90 s. The replicas were cleaned with bleach (sodium hypochlorite), washed in distilled water, mounted on uncoated copper grids and photographed in a Philips EM 300.

Static light scattering

Static light-scattering techniques are based on the Rayleigh scattering of colloidal dispersions. For unpolarized light, the normalized excess scattering per unit volume of a dispersion over that of the solvent is given by Kerker (1969):

$$R(K) = H.C.M.P_o(K)\,(1 + \cos^2\theta) \qquad (1)$$

where $K = 4\pi n/\lambda_0.\sin\theta/2$ is the scattering wave vector, θ is the angle between the scattered ray and the incident beam measured from the forward direction, M is the weight average mole weight, C is the concentration of the solute and R(K) is the Rayleigh ratio.

H is the optical constant given by:

$$H = \frac{2\pi^2 n^2 (dn/dc)^2}{N_0 \lambda_0^4} \qquad (2)$$

where n is the refractive index of the solution, dn/dc the refractive index increment with respect to solute concentration, N_0 is Avogadro's number and λ_0 the wavelength of the scattered light in vacuo.

The dimensionless function $P_0(K)$ is the particle-scattering function related to size, shape and anisotropy of the solute particles. For a rigid hollow sphere, this particle-scattering function is given by the Guinier approximation (Guinier & Fournet 1955)

$$P(K) = e^{-\frac{1}{3}R_g^2 K^2} \qquad (3)$$

where R_g is the gyration radius which is related to the optical (geometric) radius R_0. For a hollow sphere:

$$R_g^2 = \frac{3}{5} R_0^2 \frac{(1 - L^5)}{(1 - L^3)} \quad 0 \leq L < 1 \qquad (4)$$

and for a homogenous particle (L = 0):

$$R_g^2 = \frac{3}{5} R_0^2 \qquad (5)$$

Combining equations (1) and (3) yields:

$$\ln \frac{R(K)}{1 + \cos^2\theta} = \ln (HMC) - \frac{R_g^2}{3} K^2 \qquad (6)$$

From equation (6), it can be seen that in the Guinier approximation a plot of $\ln R(K)/(1 + \cos^2\theta)$ versus K^2 will give a straight line with a slope that is equal to $\frac{1}{3}R_g^2$. Consequently a modified Zimm plot was obtained by calculating the Rayleigh ratio at $K \rightarrow 0$ and $C \rightarrow 0$. The molecular weight is then given by:

$$M_w = \frac{2}{H(C/R)K \rightarrow 0 \text{ and } C \rightarrow 0} \qquad (7)$$

In our experiments, we observed that our samples probably showed some polydispersity in size. For polydisperse scattering particles P(K) may be expressed as (Alger 1979; Nugteren et al unpublished observations):

$$P(K) = \frac{\int_0^\infty \mu\, f(R)\, P_0(K)\, dR}{\int_0^\infty \mu f(R)\, dR} \qquad (8)$$

where f(R) now is the size-distribution function and $\mu = 3R^2 - 3R\delta + \delta^2$, with $\delta = R - A$ being the thickness of the spherical shell. Equation (2) is also valid for homogeneous particles (in this case one substitutes A = 0). Equation (8) was used to calculate P(K) for some hypothetical size distributions f(R) which were subsequently compared with the experimental curves from endotoxin samples. Time-averaged light-scattering experiments have been performed at wavelength λ = 546 nm with a FICA light-scattering photometer at a temperature of 25 °C. Pure benzene was used as a scattering standard, ($R_{90} = 15{\cdot}8 \times 10^{-6}$ cm^{-1} at λ_0 = 546 nm). The angular range was $30° < \theta < 150°$. Refractive index increments were measured in a Rayleigh interferometer (JENA).

Dynamic light scattering

Dynamic light scattering is used to measure the decay state of fluctuations in scattered light intensity which arise through Brownian movement. Estimates of the diffusion coefficient of the scattering particles may be made from these results.

According to the theory described by Berne & Pecora (1976), the correlation function of the scattered intensity γ (K, τ) is given by:

$$\gamma(K, \tau) \sim e^{-2Dk^2.\tau} \qquad (9)$$

From the correlation function, the diffusion coefficient D was calculated using the cumulant method (Koppel 1972). By means of the Stokes Einstein relation,

$$R_h = k_b T/6\pi\eta D, \qquad (10)$$

the hydrodynamic radius R_h was obtained; k_b being the Boltzmann constant, T, the absolute tempera-

ture and η, the viscosity of the medium. As in the case of static light scattering, the expression for the autocorrelation function will be modified when dealing with a polydisperse sample of scattering particles.

From an experimental point of view, polydispersity manifests itself when the correlation function $\gamma(K, \tau)$ is no longer a single exponential, and the diffusion coefficient, as determined by straightforward analysis of equation (9), becomes K (angle)-dependent.

The above-mentioned cumulant method can then be used to achieve an impression of polydispersity effects. Using this method, we have fitted the logarithm of the experimental correlation function to a quadratic function in time.

$$\ln \gamma (K, \tau) = a_0 + a_1\tau + a_2\tau^2 \ldots \quad (10)$$

The first cumulant, a_1 is related to the diffusion coefficient D by $D = -a_{1/2}K^2$, whereas the second cumulant, a_2, measures the deviation from non-exponential behaviour. Therefore, one often introduces a 'quality factor' or Polydispersity Index defined as

$$Q = 2a_2/a_1^2 \quad (11)$$

In the ideal, monodisperse case $Q = 0$ and values of $Q \neq 0$ indicate polydispersity effects. Dynamic light-scattering experiments were performed using an argon-ion laser (λ = 458 nm for *S. ab. equi* endotoxin and λ = 488 nm for *E. coli* and *S. marc.* endotoxin).

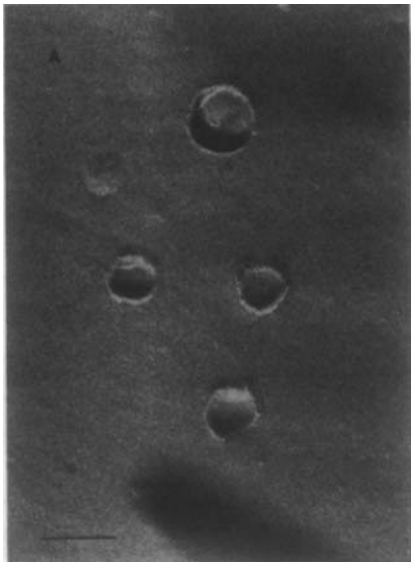

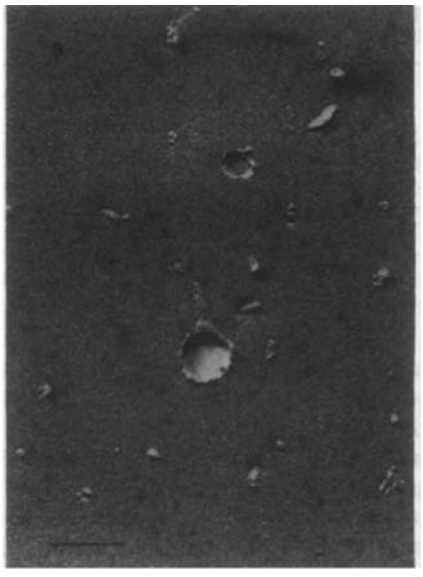

FIG. 1. Electronmicrographs of various endotoxins in water for injection: (a) *E. coli* endotoxin, (b) *S. ab. equi* endotoxin, (c) *S. marc.* endotoxin.

RESULTS

Fig. 1 shows electronmicrographs of the various endotoxin particles in water for injection. For the most part, the particles are spherical although slight distortions were seen. Similar electronmicrographs were obtained of particles in 0·1 M EDTA or 0·1 M $CaCl_2$, and after dialysis against 0·1 M EDTA for 10 days at room temperature (20 °C) to remove any

Table 1. Refractive index increments (ml g^{-1}) of endotoxins in large volume parenterals.

	E. coli	*S. ab. equi*	*S. marc.*
Water	0·144 ± 0·006	0·150 ± 0·002	0·160 ± 0·001
EDTA 0·1 M	0·127 ± 0·007	0·135 ± 0·004	0·138 ± 0·013
$CaCl_2$ 0·1 M	0·140 ± 0·016	0·133 ± 0·004	0·151 ± 0·002
NaCl 0·9%	0·139 ± 0·014	0·145 ± 0·004	0·160 ± 0·011
Dextrose 5%	0·139 ± 0·011	0·164 ± 0·016	0·150 ± 0·011
Ringer's	0·149 ± 0·003	0·149 ± 0·007	0·162 ± 0·005
Vamin-N	0·135 ± 0·017	0·153 ± 0·027	0·142 ± 0·006
Isodex	0·140 ± 0·016	0·176 ± 0·006	0·158 ± 0·013

residual divalent cations. Particle radii were predominantly in the range 10–100 nm which agree with the light-scattering data in Table 2.

Examples of Guinier plots (7) are shown in Fig. 2. The relatively strong curvature in the 0·1 M EDTA data, indicates a pronounced heterodispersity of the particles compared with the $CaCl_2$ data. Table 1 shows the refractive index increments of the various endotoxins. The results of the light-scattering data are shown in Table 2.

Although the observed polydispersity does not impede comparison of the behaviour of endotoxins in different environments, it does hamper an accurate quantitative analysis with respect to particle size. To get an impression of the effect of polydispersity on the results using Guinier's approximation for particle-size characterization, we calculated the generalized scattering function P(K) versus K^2 by a numerical integration of equation (8) for hypothetical size distributions. These calculations were carried out for homogenous spheres, i.e. by taking L = 0 (eq 4) and for two different size distributions, namely a normal (Gaussian) distribution and a log-normal distribution.

For the normal distribution (i.e. $f(R) = \exp[-(R - \bar{R})^2]/2\sigma^2$), we used a mean radius $\bar{R}_0$ = 70 nm and a standard deviation σ = 30 nm. As Fig. 3 shows, no deviations from linearity in ln (P(K)) versus K^2 were observed for this distribution. On application of linear least squares fit to this ln (P(K)) versus K^2 plot, we obtain a gyration radius R_g = 83 nm using equation (3) and consequently, using equation (5), an optical radius R_0 = 107 nm. If this last value is compared with the starting point for the calculations, i.e. a mean optical radius $\bar{R}_0$ = 70 nm, it is seen that there is a an overestimation of the mean particle size when a straight-forward Guinier analysis is applied to experimental data from a polydisperse sample.

Fig 3 also shows the results of the calculations using a log-normal distribution, i.e. $f(R) = \exp([-(\log R - \log \bar{R})^2]/2\sigma_g^2)$ with a mean radius $\bar{R}_0$ = 50 nm and a geometric standard deviation σ_g = 0·25. In this case, there is a clear curvature in the Guinier plot. From the slope of a linear least squares fit, we now obtain a gyration radius R_g = 83 nm and an optical (geometrical) radius R_0 = 107 nm. Although a linear least squares fit is questionable in the latter case, again there is an overestimation of the mean particle radius. On comparison of the experimental curves in Fig. 2 with the log-normal distribution curve in Fig. 3, there is a striking similarity which suggests that endotoxin dispersions comprise a heterodisperse population following a log-normal distribution. This is supported by the size-distribution histogram, obtained by freeze-etch electronmicroscopy, of one of the *S. abortus equi* endotoxin lots shown in Fig. 4, which also shows a mean geometrical radius less than half the value computed from light-scattering experiments.

Table 2. Data from static light-scattering experiments using Guinier's approximation uncorrected for polydispersity.

	E. coli			*S. ab. equi*			*S. marc.*		
Medium	$R_{k\to0}$	R_o	M_w	$R_{k\to0}$	R_o	M_w	$R_{k\to0}$	R_o	M_w
Water	0·184	105 ± 2	1·4	0·062	84 ± 3	0·4[a]	0·030	88 ± 6	0·2
				0·026	51 ± 2	0·2[b]			
EDTA 0·1 M	0·019	84 ± 1	0·2	0·030	87 ± 1	0·3	0·017	76 ± 1	0·1
EDTA 0·1 M dialysed	0·014	91	—	0·024	108	—	0·016	76	—
$CaCl_2$	0·159	102 ± 1	1·3	0·095	92 ± 1	0·8	0·017	82 ± 1	0·1
NaCl 0·9%	0·037	90 ± 3	0·2	0·048	87 ± 2	0·2	0·021	87 ± 1	0·2
Dextrose 5%	0·104	94 ± 2	0·4	0·054	80 ± 1	0·3	0·022	83 ± 1	0·1
Ringer's	0·124	99 ± 1	0·8	0·061	80 ± 1	0·4	0·038	87 ± 1	0·2
Vamin-N	0·079	97 ± 1	0·5	0·048	86 ± 1	0·4	0·014	78 ± 1	0·1
Isodex		n.d.		0·040	79 ± 4	0·2	0·020	72 ± 2	0·1

$R_{k\to0}$ (10^{-3} cm^{-1}): Calculated from solutions containing 100 μg ml^{-1}.
R_o (nm): Mean ± s.e.m., 5 concentrations.
M_w ($\times10^8$): From $R_{k\to0 \text{ and } c\to0}$.
EDTA 0·1 M dialysed: Data from one sample containing 100 μg ml^{-1}.
[a,b] Data from two different lots.

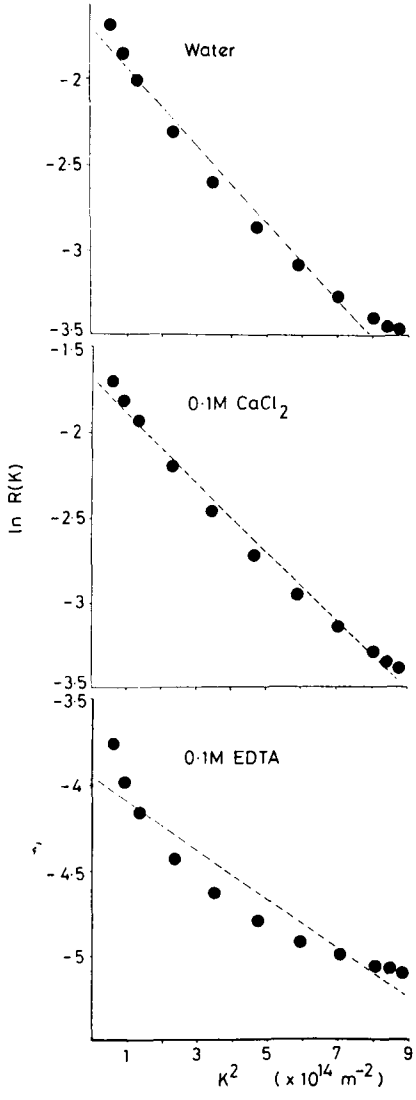

FIG. 2. Typical Guinier plots for endotoxin dispersions: *E. coli* endotoxin 100 μg ml^{-1} in water, *E. coli* endotoxin 100 μg ml^{-1} in 0·1 M $CaCl_2$, *E. coli* endotoxin 100 μg ml^{-1} in 0·1 M EDTA.

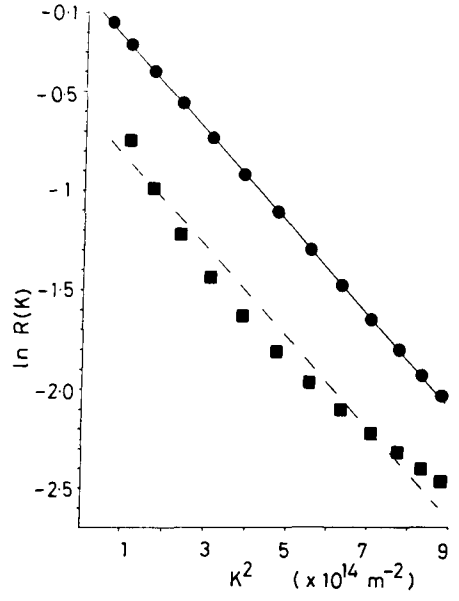

FIG. 3. Calculated Guinier plots for hypothetical size distributions. ●, normal distribution, $\bar{R}_0$ = 70 nm, σ = 30 nm; ■, log-normal distribution, $\bar{R}_0$ = 50 nm, σ = 25 nm.

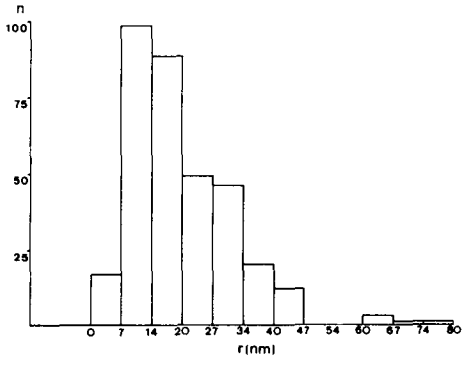

FIG. 4. Size-distribution histogram of *S. ab. equi* endotoxin (lot b) in water, obtained by freeze-etch electronmicroscopy.

Table 3. Data from dynamic light-scattering experiments of endotoxins in water for injections.

	E. coli	*S. ab. equi**	*S. marc.*
Diffusion coefficient (10^{-12} m s^{-1})[a]	2·45 ± 0·19	4·10 ± 0·13	2·47 ± 0·07
Hydrodynamic radius (nm)[a]	108·0 ± 13·0	60·0 ± 2·0	99·0 ± 3·0
Polydispersity index[b]	0·15 ± 0·02	0·07 ± 0·01	0·10 ± 0·01

[a] Data represent mean ± s.e.m. of 4 different concentrations (20–100 μg ml^{-1} for *E. coli* and *S. ab. equi*, 100–500 μg ml^{-1} for *s. marc.*).

[b] Measured at 5 different angles at a concentration of 100 μg ml^{-1}. Data represent mean ± s.e.m.

* Lot b.

These calculations indicate that care is needed in the interpretation of light-scattering data shown in Table 2, the real optical radii probably being half the value shown. Unfortunately, the influence of polydispersity on the molecular-mass determination is difficult to evaluate, partly due to the fact that the radii are Z-averaged, whereas the molar masses are weight-averaged.

The relevant data from the dynamic light-scattering experiments are shown in Table 3. Agreement is seen between optical radii from Table 1 and

the hydrodynamic radii from Table 3. A substantial polydispersity index ('quality factor') confirms the polydisperse character of endotoxin dispersions.

DISCUSSION

The configurational aspects of endotoxins have been subject to various conflicting studies. Schramm et al (1952) describe chain-like aggregation states of spherical subunits, but suggest that their formation is possibly a consequence of the drying process between negative staining and electronmicroscopy. Beer et al (1966) describe sheet and spherical particles resembling our own data. Ribi et al (1966) describe long and short filaments, dissociating upon the addition of sodium deoxycholate, whereas DePamphilis (1971) found large vesicular aggregates (20–40 μm) which dissociated into discs of 14–70 nm and rods (10–20 nm long) upon dialysis against Tris-EDTA buffer. These discrepancies might result from different bacterial strains, extraction procedures or electonmicroscopic procedures. More uniformity exists among the subunits of these aggregates which are thought to be dimeric, amphilic subunits with a molecular mass of approximately 20 000 (Hannecart-Pokorni et al 1973; Shands & Chun 1980). They consist of a central lipophilic part and two diametrical hydrophilic chains, their total length being estimated at 20–70 nm long and diameter 1 nm, depending on bacterial strain. Electronmicroscopic procedures imply negative staining and/or drying, both of which might profoundly affect particle characteristics. In this study, freeze-etch electronmicroscopy of endotoxins was used and clearly showed spherical particles. The instantaneous freezing ensures the absence of particle distortion. The same type of particle was seen in the absence or presence of $CaCl_2$ after dialysis against 0·1 M EDTA. These particles resemble the artificially prepared vesicles from phosphatidylcholine (Kremer et al 1977) or dipalmitoylphosphatidylcholine (van Venetie et al 1980).

The occurrence of globular particles independent of the medium used also appears from the light-scattering results. In the case of *S. abortus equi* and *S. marcescens* calcium addition or depletion has little influence on the particle sizes. This is confirmed by correspondingly small changes in opalescence as expressed by the $R_{k \to 0}$ values. Only *E. coli* endotoxins appear to be affected by the absence of Ca^{2+} ions, a maximal particle size being observed in water, 0·1 M $CaCl_2$ or Ringer solution with corresponding high $R_{K \to 0}$ values. *E. coli* endotoxin in 0·1 M EDTA shows a sharp drop in opalescence, particle size and molecular weight while polydispersity is increased (see Fig. 1).

The overall picture that emerges from Table 2 is that there are no great differences between the particle characteristics of endotoxins in various infusion fluids such as strongly ionogenic media (e.g. NaCl 0·9%) or non-ionogenic media (dextrose 5%). However, these two media show different properties with respect to endotoxin removal or endotoxin detection.

The fact that the particle sizes of both *S. abortus equi* and *S. marcescens* endotoxins are hardly influenced by the presence or absence of Ca^{2+} ions whereas that of *E. coli* endotoxin is, indicates the properties of endotoxins vary with their origin. A similar result is described by Shands & Chun (1980), who examined endotoxins of three different strains of *S. typhimuri*, and found one of the strains to show no qualitative change in endotoxin morphology after EDTA treatment. Not only different bacterial strains, but also different preparations of one endotoxin might show substantial differences, as is indicated by the difference in particle size of two lots of *S. abortus equi* endotoxin used in this study (one of these lots was tested in water only).

We also found different molecular masses for the various endotoxins with *E. coli* endotoxin showing the greatest particle masses. These particle masses are of the same order as those of liposomes with comparable radii prepared by various methods (Kremer et al 1977; Zumbuehl & Weder 1981), assuming the real geometric radii to be half the values mentioned in Table 1. Although we do not know the exact relevance of polydispersity effects for molar-mass determinations, these molar masses are substantially higher than those from endotoxin molar-mass data described so far (Ribi et al 1966; Schramm et al 1952) which suggest a particle mass of 10^6 daltons.

The ultimate structure of the particles is not indicated by this study. The spherical shape allows two possible conformations to exist: a vesicular structure surrounding a central, water-filled cavity or a homogenous, dense particle. Our calculations were based on the latter model. We also attempted to establish the charge on the endotoxin particles using micro-electrophoresis with visible or laser light. Unfortunately, in both cases the particles remained invisible.

The concentrations used in this study are substantially higher than those usually encountered in large volume parenterals, so endotoxins might behave

differently at different concentrations. But so far there has been no evidence for this.

We believe that only minor differences in particle size occur among endotoxins existing in various infusion fluids. Furthermore, these differences do not agree with the observed differences in LAL-CS detection or removal by depth filtration, thereby ruling out changes in aggregation state as a possible cause for different behaviour. To explain the depth filtration differences, attention should be focused on other endotoxin parameters, and since such filtration is governed primarily by electrokinetic phenomena, a shift in the zetapotential of the particles could be the explanation. A similar shift is described for a phospholipid-stabilized soybean-oil emulsion used in parenteral nutrition (Dawes & Groves 1978).

Acknowledgements

The authors wish to acknowledge H. J. Mos for carrying out most of the dynamic light-scattering experiments, D. M. Wisse for technical assistance during freeze-etch electronmicroscopy, and Dr J. A. Loos for his valuable suggestions in the preparation of the manuscript. This study was supported by a grant from NPBI Laboratories, Emmer Compascuum, The Netherlands.

REFERENCES

Alger, T. W. (1979) Applied Optics 18: 3494–3501

Baggerman, C., Brandsema, C., Humer, M., Visser, J. (1981) J. Pharm. Pharmacol. 33: 685–691

Baggerman, C., Kannegieter, E. M. (1984) Appl. Env. Microbiol. 48: 662–664

Beer, E., Braude, A. I., Brinton, C. C. (1966) Ann. N.Y. Acad. Sci. 166: 450–475

Berne, B. J., Pecora, R. (1976) Dynamic Light Scattering with Applications to Chemistry, Biology and Physics. Wiley & Sons, New York

Dawes, W. H., Groves, M. J. (1978) Int. J. Pharm. 1: 141–150

DePamphilis, M. L. (1971) J. Bacteriol. 105: 1184–1189

Guinier, A., Fournet, G. (1955) Small angle scattering of X-rays. Wiley & Sons, New York

Hannecart-Pokorni, E., Dekegel, D., Depuidt, F. (1973) Eur. J. Biochem. 38: 6–13

Kannegieter, E. M., Baggerman, C. (1984) J. Par. Sci. Technol. in press

Kerker, M. (1969) Scattering of light and other electromagnetic radiation. Academic Press, New York

Koppel, D. E. (1972) J. Chem. Physics 57: 4814–4821

Kremer, J. M. H., Van den Esker, M. W. J., Pathmamanoharan, C., Wiersema, P. H. (1977) Biochemistry 16: 3932–3952

Maki, P. G. (1976) in: Phillips, I., Meers, P. D., d'Arcy, P. F. (eds) Microbial growth in infusion fluids; Microbiological Hazards of Infusion Therapy. MTP Press Ltd, Lancaster

Ribi, E., Anacker, R. L., Brown, R., Haskins, W. T., Malmgren, B., Milner, K. C., Rudbach, J. A. (1966) J. Bacteriol. 92: 1493–1509

Schramm, G., Westphal, O., Lüderitz, O. (1952) Z. Naturforsch. (B) 7B: 594–598

Shands, J. W., Chun, P. W. (1980) J. Biol. Chem. 255: 1221–1226

Sweadner, K. J., Forte, M., Nelsen, L. L. (1977) Appl. Env. Microbiol. 34: 382–385

Tsuji, K., Steindler, K. A. (1983) Appl. Environm. Microbiol. 45: 1342–1350

van Venetie, R., Vervegart, H. J. T., Verkley, A. J., Van Deenen, L. L. M. (1980) J. Microscopy 118: 401–408

Wisse, D. M., Spies, F. (1981) Ibid. 127: 227–231

Woog, H., Krüger, D., Zimmermann, G. (1977) Pharm. Ind. 39: 1261–1266

Zumbuehl, O., Weder, H. G. (1981) Biochim. Biophys. Acta 640: 252–262